FULL PAPER

Dye-sensitized solar cells using silicon phthalocyanine photosensitizers with pyridine anchor: Preparation, evaluation of photophysical, electrochemical, and photovoltaic properties

Emre Güzel[1] [ID] | Hüseyin Baş[2] [ID] | Zekeriya Biyiklioglu[2] [ID] | İlkay Şişman[3] [ID]

[1]Department of Fundamental Sciences, Sakarya University of Applied Sciences, Sakarya, Turkey

[2]Department of Chemistry, Karadeniz Technical University, Trabzon, Turkey

[3]Department of Chemistry, Sakarya University, Sakarya, Turkey

Correspondence
Zekeriya Biyiklioglu, Department of Chemistry, Karadeniz Technical University, Trabzon, Turkey.
Email: zekeriyab@ktu.edu.tr

In this study, novel two silicon phthalocyanine photosensitizers (**3PY-Si** and **4PY-Si**) containing pyridine groups as an electron-withdrawing and anchoring group have been prepared and chemically characterized for dye-sensitized solar cells (DSSCs). Photoelectrochemical and photovoltaic properties of the photosensitizers were evaluated. The new photosensitizers elucidated by spectroscopic and electrochemical techniques. As reported by fluorescence measurements, the silicon phthalocyanine photosensitizers exhibited slightly higher fluorescence quantum yield ($\Phi_F = 0.25$) than the unsubstituted zinc phthalocyanine which is favorable for photophysical applications. The DSSC based on complex **3PY-Si** shows the highest power conversion efficiency (PCE) of 0.53% with the J_{sc}, V_{oc} and FF values of 1.205 mA cm^{-2}, 0.612 V, and 0.72, respectively, in the presence of the coadsorbent. These silicon phthalocyanine photosensitizers with bulky axial pyridine substituents found to be important materials for (DSSCs) since they show strong absorption in the red region and their ligands hamper the stacking of rings. This situation prevented the formation of aggregates with a common tendency to photosensitizers on the TiO$_2$ surface.

KEYWORDS
dye-sensitized solar cells, photosensitizer, phthalocyanine, pyridine anchor, silicon

1 | INTRODUCTION

Owing to growing global energy, technological developments and increasing use of electronic equipment, energy conversion has become very important in our lives. Many advanced studies have been done by scientists to have this transformation. One of the works that have been done by the scientist is dye-sensitized solar cells (DSSC), which are actively used in photovoltaic technology. DSSC performance depends on the formation of the sensitizers used, the photoanode, the counter-electrode, the electrolyte used, and the harmonious operation of all these equipment.[1,2] It works with the addition of electrolyte

between the photoanode coated with TiO$_2$ and the counter electrode and the transfer of electrons in this closed system. The efficiency of electron transfer of dyes is also related to the structure of the dye. DSSCs using ruthenium complexes as dyes yielded 11.5% power conversion efficiency (PCE) under AM 1.5G irradiation.[3] However, the low absorption coefficient of these ruthenium sensitizers in the red region and the low availability of ruthenium has led to the development of effective and ruthenium-free sensitizers for DSSCs. In contrast to ruthenium dyes, phthalocyanine (Pc) dyes, which are sensitizers with extended π-conjugation, have attracted attention owing to high absorption coefficients in the red

region of the solar spectrum and efficient photo-induced electron transfer.[1,4,5] These dyes exhibited high performance in DSSC applications with light-harvesting efficiency up to 700 nm and good photochemical and thermal stability properties.[1,6,7] This makes them attractive for DSSCs. Due to the planar structure of the Pc ring, Pcs which do not contain substituents or contain bulky substituents have a high tendency to aggregate.[8,9] To prevent aggregation, bulky axial or equatorial substituents may be added to the phthalocyanine structure.[4,9–13] In this sense, the axially ligated hexacoordinate nature of silicon phthalocyanines is important because the axial substituents can not only hinder undesired dye aggregation on the TiO_2 surface but also can increase the solubility of Pcs in many organic solvents.[13–15]

The anchoring groups in DSSCs, such as carboxylic acid, cyanoacrylic acid or rodanin-3-acetic acid which generally serve as electron acceptors, are used to ensure that the dye attaches to the semiconductor surface.[16,17] The carboxylic acid groups form a strong ester linkage with the semiconductor surface, providing a strong electronic communication between the dye and the semiconductor surface.[1] However, using different functional groups as an anchor and electron acceptor can enable the development of new dyes for DSSCs.[6] In this study, in order to prepare new and efficient phthalocyanine photosensitizers in DSSCs, different dyes with a stronger interaction between the electron-accepting moiety of the sensitizers and the TiO_2 surface can be designed. In this manner, we prepared two silicon photosensitizers and tested the utility of a pyridine ring as an electron-withdrawing and anchoring group in place of a conventional carboxy group in phthalocyanine-sensitized solar cells. Also, their electrochemical, photophysical, and photovoltaic properties were examined.

2 | EXPERIMENTAL

The used materials, equipment, electrochemical, photophysical, photovoltaic parameters, and characterization details were supplied as Supplementary information.

2.1 | Synthesis

2.1.1 | Bis-[(3-pyridin-3-ylpropoxy)] phthalocyaninato silicon (IV) (3PY-Si)

A mixture of 3-pyridinepropanol (**3PY-OH**) (0.06 mL, 0.48 mmol), SiPcCl$_2$ (0.15 g, 0.24 mmol), NaH (0.011 g, 0.48 mmol) was refluxed in dried toluene (15 mL) at 110°C for 24 hr. Then the solvent was evaporated and the

crude product was purified by aluminum oxide column chromatography using CHCl$_3$:MeOH (100:1). Yield: 50 mg (25%), m.p. > 300°C. IR (ATR), ν/cm^{-1}: 3022 (Ar-H), 2,917–2,848 (Aliph. C-H), 1519, 1472, 1445, 1427, 1351, 1333, 1290, 1253, 1165, 1121, 1106, 1075, 955, 909, 758, 729. ^{1}H-NMR (400 MHz, CDCl$_3$), (δ): 9.67 (s, 8H, Pc-H$_\alpha$), 8.38 (s, 8H, Pc-H$_\beta$), 7.95 (s, 2H, Ar-H), 7.12 (s, 2H, Ar-H), 6.49 (bs, 2H, Ar-H), 5.82 (m, 2H, Ar-H), −0.12 (bs, 4H, Ar-CH$_2$), −1.28 (bs, 4H, -CH$_2$-), −2.03 (bs, 4H, Si-O-CH$_2$). ^{13}C-NMR (100 MHz, CDCl$_3$), (δ): 149.28, 148.66, 146.09, 136.30, 135.93, 134.74, 130.97, 123.72, 122.24, 53.78, 30.15, 29.70. UV–Vis (CHCl$_3$) λ_{max} nm (log ε): 673 (5.23), 644 (4.43), 606 (4.46), 355 (4.77). MALDI-TOF-MS m/z calc. 812.95; found: 812.17 [M]$^+$.

2.1.2 | Bis-[(4-pyridin-3-ylpropoxy)] phthalocyaninato silicon (IV) (4PY-Si)

4PY-Si was synthesized similarly to **3PY-Si** by using 4-pyridinepropanol (**4PY-OH**). The crude product was purified by aluminum oxide column chromatography using CHCl$_3$:MeOH (100:2). Yield: 93 mg (47%), m.p. > 300°C. IR (ATR), ν/cm^{-1}: 3055 (Ar-H), 2941–2866 (Aliph. C-H), 1599, 1520, 1446, 1427, 1334, 1291, 1215, 1165, 1123, 1096, 1079, 1059, 957, 910, 759. ^{1}H-NMR (400 MHz, CDCl$_3$), (δ): 9.66 (bs, 8H, Pc-H$_\alpha$), 8.37 (bs, 8H, Pc-H$_\beta$), 7.78 (m, 4H, Ar-H), 5.50 (m, 4H, Ar-H), −0.09 (bs, 4H, Ar-CH$_2$), −1.30 (bs, 4H, -CH$_2$-), −2.12 (bs, 4H, Si-O-CH$_2$). ^{13}C-NMR (100 MHz, CDCl$_3$), (δ): 149.29, 149.26, 148.30, 135.91, 131.04, 123.73, 122.80, 53.45, 29.68, 29.12. UV–Vis (CHCl$_3$) λ_{max} nm (log ε): 674 (5.45), 645 (4.64), 607 (4.69), 354 (4.99). MALDI-TOF-MS m/z calc. 812.95; found: 812.70 [M]$^+$.

3 | RESULTS AND DISCUSSION

3.1 | Synthesis and characterization

The synthesis of pyridine substituted silicon phthalocyanines (**3PY-Si, 4PY-Si**) is given in Scheme 1. Bis-[(3-pyridin-3-ylpropoxy)]phthalocyaninato silicon (IV) and bis-y[(4-pridin-3-ylpropoxy)]phthalocyaninato silicon (IV) were synthesized by the reaction of SiPcCl$_2$ with 3-pyridinepropanol (**3PY-OH**), 4-pyridinepropanol (**4PY-OH**), in the presence of NaH in toluene. **3PY-Si** and **4PY-Si** were elucidated by a combination of methods including FT-IR, ^{1}H-NMR, ^{13}C-NMR, UV–Vis, and MALDI-TOF MS.

In FT-IR spectra, the structure of bis-[(3-pyridin-3-ylpropoxy)]phthalocyaninato silicon (IV) **3PY-Si** and bis-[(4-pyridin-3-ylpropoxy)]phthalocyaninato silicon (IV)
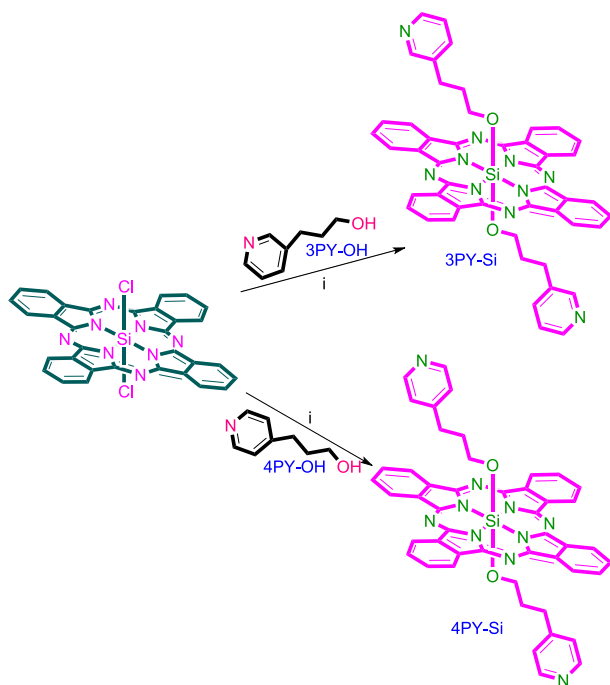
SCHEME 1   The synthesis of pyridine substituted silicon phthalocyanines. (i) Toluene, NaH, 120°C

FIGURE 1   FT-IR spectra of dye powders (red line) and dye adsorbed onTiO$_2$ (blue line) for dye 4PY-Si

4PY-Si were confirmed by the vibration of Si-O bond at 1075 and 1,079 cm^{-1}, respectively.

Figure 1 exhibits the FT-IR spectra of the 4PY-Si powder and the 4PY-Si adsorbed on TiO$_2$. When the FT-IR spectrum of 4PY-Si adsorbed on TiO$_2$, the new band raised at around 1609 cm^{-1}, which is confirmed to the pyridine ring coordinated to the Lewis acid areas of the semiconductor TiO$_2$ surface.[18–20] This band shows that the 4PY-Si is chiefly adsorbed on the TiO$_2$ surface by coordinate bonding at the Lewis acid areas (from nitrogen atoms to Ti^{n+} cations). The bathochromic shift of the absorption maximum shows that the absorbed dye occurs a coordination bond on the TiO$_2$ surface. The coordination bond formed between the Lewis region of the TiO$_2$ surface and the pyridine ring of the photosensitizer indicates that the pyridine ring may be a candidate for electron-withdrawing anchoring groups in DSSCs.

In the ^{1}H-NMR spectra, the H$_\alpha$ protons of 3PY-Si and 4PY-Si appeared at 9.67 and 9.66 ppm, the H$_\beta$ protons of 3PY-Si and 4PY-Si appeared at 8.38 and 8.37 ppm. The protons of Ar-CH$_2$, -CH$_2$- and Si–O–CH$_2$ shifted negative [(−0.12)-(−2.03) ppm] for 3PY-Si (Figure 2A) and [(−0.09)-(−2.12) ppm] for 4PY-Si owing to the magnetic anisotropy of the Pc ring.[21] Also, ^{13}C-NMR spectra supported the 3PY-Si (Figure 2B) and 4PY-Si structures. In the MALDI-TOF MS spectra of 3PY-Si and 4PY-Si, molecular ion peaks at m/z 812.17 [M]$^+$, 812.70 [M]$^+$ are in accordance with the calculated values, respectively (Figure S1).

3.2 | UV–vis studies
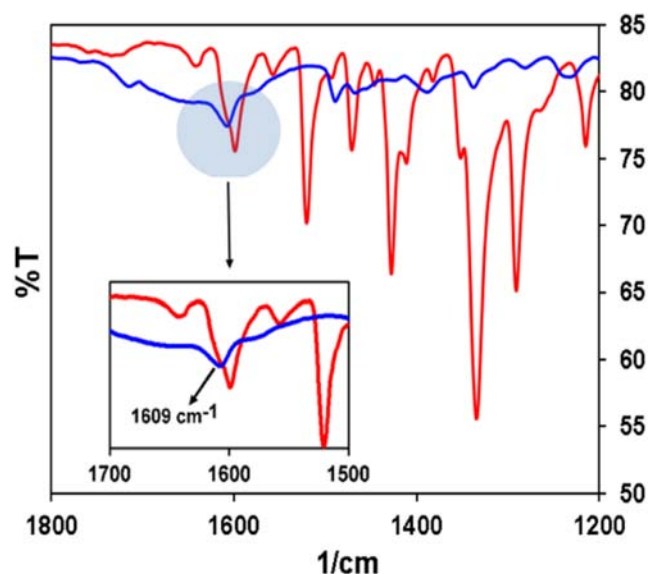
The UV–Vis absorption spectra of the phthalocyanine photosensitizers (3PY-Si and 4PY-Si) in CHCl$_3$ as the non-coordinated solvent is exhibited in Figure 3. The intense and sharp well-defined Q-band centered at 673 and 674 nm exhibits the lack of aggregation phenomena in the solution. This situation is quite important for important sensitization of the material.

In this study, aggregation behaviors of 3PY-Si and 4PY-Si were examined by UV–Vis spectrophotometer in different solvents and concentrations. Figure S3A shows the UV–Vis spectra of the 3PY-Si in different organic solvents. 3PY-Si and 4PY-Si did not show any aggregation in DMSO, THF, DMF, CHCl$_3$, EtOAc, and CH$_2$Cl$_2$ owing to axial substitution (Figures S2A and S3A). Also, aggregation behaviors of the 3PY-Si and 4PY-Si were investigated at different concentrations in DMSO. No aggregation tendency has been demonstrated for 3PY-Si (Figure S3B) and 4PY-Si (Figure S2B). Because a steady increase in the intensity of the spectra was shown with increasing concentration. This increase was compatible with the Beer–Lambert law.

UV/Vis spectroscopy of the photosensitizer adsorbed on TiO$_2$ nanoparticles exhibits that the photosensitizer 4PY-Si was adsorbed onto the TiO$_2$ without chenodeoxycholic acid (CDCA) as a co-adsorbent, Q-band absorption maximum red-shifted by about 5 nm compared to that in the CHCl$_3$ (Figure 4). The red-shifted of the Q-bands is owing to the interaction between the anchor group of the photosensitizer and the mesoporous
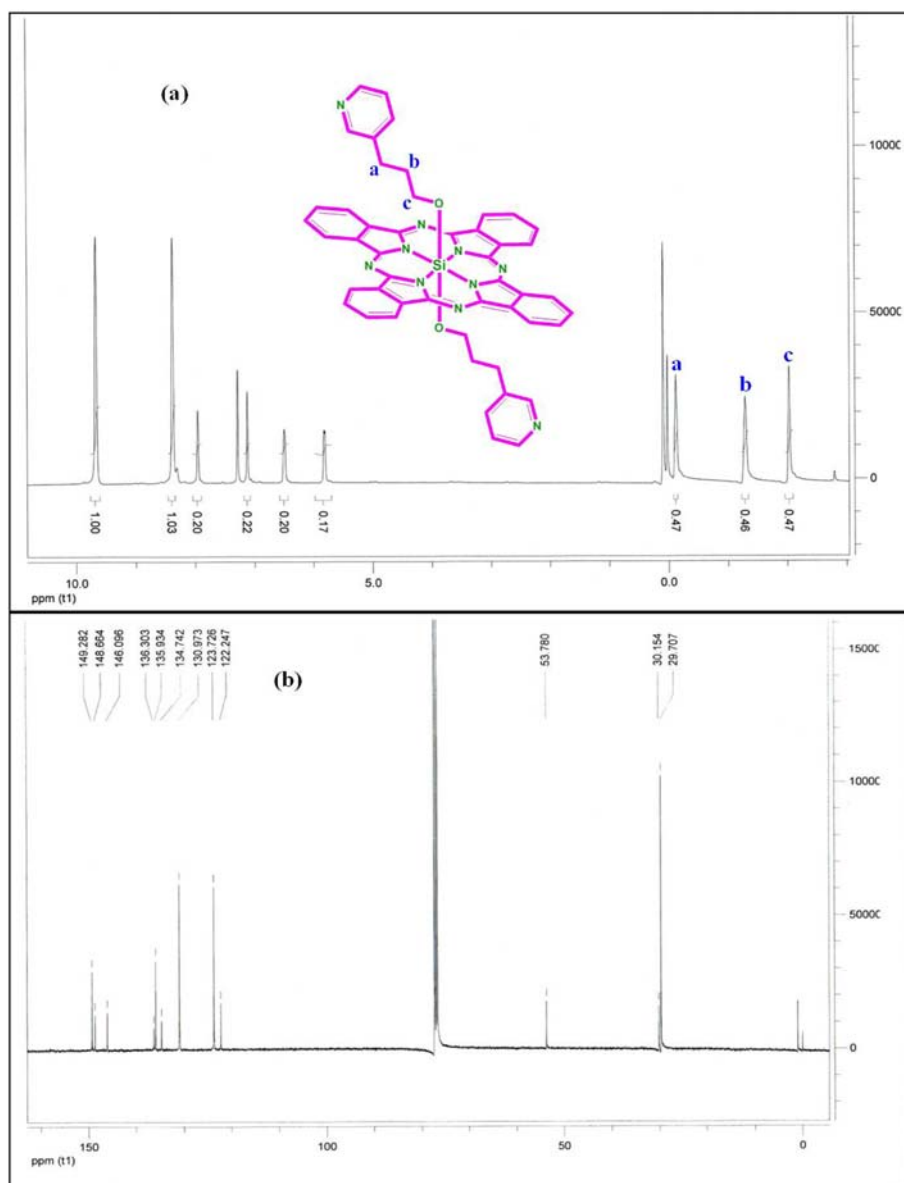
FIGURE 2 (A) ^{1}H-NMR spectrum of **3PY-Si**. (B) ^{13}C-NMR spectrum of **3PY-Si**

TiO$_2$ surface. This is owing to the strong interaction between the pyridine and the TiO$_2$ surface of the pyridine containing the electron-withdrawing anchoring group.[19,22] Also, the solid-state spectrum of **3PY-Si** and **4PY-Si** adsorbed onto titania displays a broadening of the phthalocyanine Q-band. This slight enlargement is chiefly owing to the adsorption of the photosensitizer molecules onto the semiconductor surface (TiO$_2$). On the other hand, the interaction of 3-pyridin-3-ylpropoxy moiety and TiO$_2$ surface, in cases with and without CDCA, the absorption spectra of the photosensitizer **4PY-Si** indicate minimal or no aggregation, showing that the aggregation could be expeditiously hampered by the steric effect of flexible and long axial 3-pyridin-3-ylpropoxy group in the molecule (Figure 4 inset). Similar behavior was also observed for photosensitizer **3PY-Si**.

3.3 | Photophysical studies

Determining the fluorescence behavior and fluorescent quantum efficiencies of a photosensitizer are the basis of its photophysical properties.[4] In this manner, the fluorescence excitation, emission, and absorption spectra of silicon di-substituted phthalocyanine photosensitizers **3PY-Si** (Figure 5) and **4PY-Si** (Figure S4) investigated and these complexes exhibited similar fluorescence behavior in THF. The UV–vis absorption, excitation, emission, and fluorescence quantum yield (Φ_F) of **3PY-Si** and **4PY-Si** are summarized in Table 1.

Fluorescence quantum yield was determined using the comparative method. ZnPc in THF ($\Phi_F = 0.23$) was used as the standard.[23] Fluorescence emission maxima were detected at 694 nm for photosensitizer **3PY-Si**, at
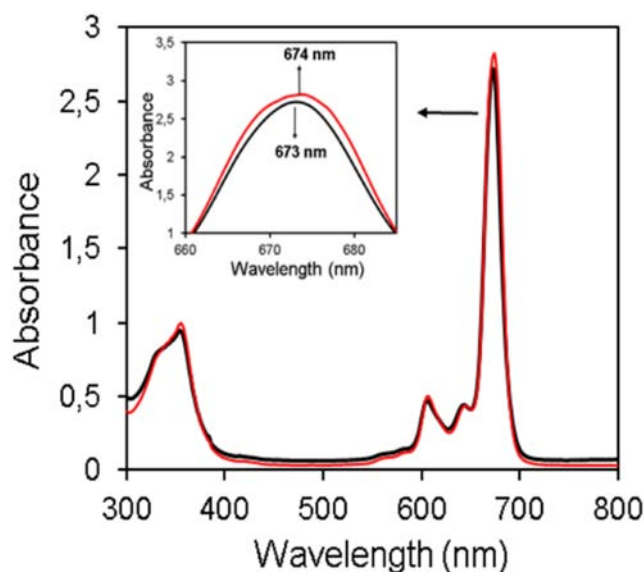
FIGURE 3 UV–Vis absorption spectra of **4PY-Si** (red line) and **3PY-Si** (black line) in CHCl$_3$
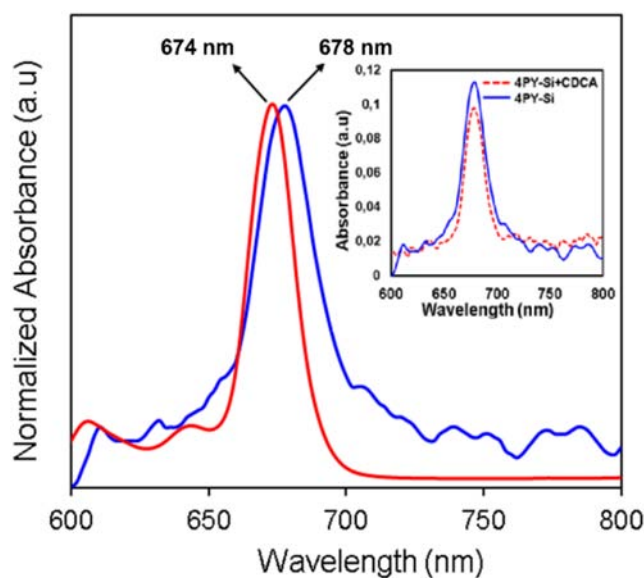

FIGURE 4 UV–Vis absorption spectra of **4PY-Si** in CHCl$_3$ solution (red line), on TiO$_2$ film (blue line). The inset shows UV–Vis absorption spectra of **4PY-Si** with and without 1 mM chenodeoxycholic acid (CDCA) on TiO$_2$ film

683 nm for compound **4PY-Si** in THF. The excitation spectra are similar to the absorption spectra and these spectra are mirror images of the emission spectra for the silicon phthalocyanine photosensitizer s **3PY-Si** and **4PY-Si** in THF. This fact reveals that axial substitution has a small or negligible effect on the spectroscopic properties of SiPcs. Fluorescence results exhibited that the silicon photosensitizers exhibited a slightly higher fluorescence quantum yield ($\Phi_F = 0.25$) than the
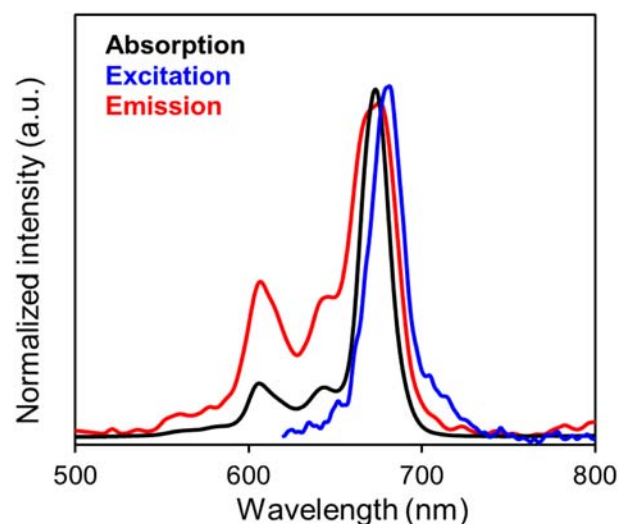

FIGURE 5 Electronic absorption, excitation and fluorescence emission spectra of **3PY-Si** in THF. (Excitation wavelength = 682 nm)

unsubstituted zinc phthalocyanine owing to relatively less aggregation in THF.[24]

3.4 | Electrochemical studies

Electrochemistry of **3PY-Si** and **4PY-Si** was investigated using cyclic voltammetry (CV) in dichloromethane at room temperature (DCM)/tetrabutylammoniumperchlorate (TBAP) electrolyte system on a Pt working electrode. Zero–zero band gap energy (E_{0-0}) was determined from the intersection of the normalized absorption spectra.[25] The oxidation and reduction potentials are summarized in Table 2. Figure 6 shows the CV responses of **3PY-Si** and **4PY-Si**. These photosensitizers show two reversible reduction potentials (R$_1$ = −0.70 V, R$_2$ = −1.18 V for **3PY-Si**, R$_1$ = −0.72 V, R$_2$ = −1.25 V for **4PY-Si**) which assigned to the phthalocyanine ring. Besides, **3PY-Si** and **4PY-Si** show one quasi-reversible oxidation potentials (O$_1$ = 1.23 V for **3PY-Si,** O$_1$ = 1.35 V for **4PY-Si**). The HOMO levels of **3PY-Si** and **4PY-Si**, estimated from the oxidation potential, are located at 1.12 and 1.24 V, respectively. This result shows that **3PY-Si** oxidizes more easily than **4PY-Si**.

The HOMO levels of the photosensitizers **3PY-Si** and **4PY-Si** are more positive than that of I$^-$/I$_3^-$ (0.4 V vs. NHE), ensuring the efficient dye regeneration. The LUMO levels were obtained as −0.65 and −0.53 V from the HOMO and the E_{0-0}. These values are more negative than the conduction band (CB) of TiO$_2$ (−0.5 V vs. NHE), suggesting that the photosensitizers can inject electrons to TiO$_2$ (Figure S5).[26]

TABLE 1 Electrochemical and optical properties of photosensitizers **3PY-Si** and **4PY-Si**

Dye	λ_{abs} [nm][a] (ε [x 10^5 M^{-1} cm^{-1}][a])	λ_{onset} [nm][a]	λ_{em} [nm][a]	λ_{ex} [nm][a]	λ_{abs} (TiO_2) [nm][b]	Φ_F[c]	E_{0-0} [eV][d]	E_{ox} [V][e]	E_{HOMO} [V][f]	E_{LUMO} [V][g]
3PY-Si	673 (2.27)	699	682	674	678	0.24	1.77	0.49	1.12	−0.65
4PY-Si	674 (2.34)	698	683	675	678	0.25	1.77	0.61	1.24	−0.53
ZnPc[c]	666	–	673	666	–	0.23	–	–	–	–

[a]λ_{abs}: absorption wavelength; λ_{onset}: absorption onset wavelength; λ_{em}: emission wavelength, λ_{ex}: excitation wavelength.

[b]λ_{abs} (TiO_2): absorption maximum wavelength on the TiO_2 film.

[c]Φ_F: fluorescence quantum yields (using unsubstituted ZnPc in THF as the reference[23]).

[d]E_{0-0}: bandgap, obtained utilizing the equation $E_{0-0} = 1240/\lambda_{onset}$.

[e]E_{ox}: oxidation potential (O_1), referred to the external Fc/Fc$^+$ standard (0.74 V vs. SCE).

[f]E_{HOMO} (vs. NHE) was obtained by the addition of 0.63 V to the E_{ox}.

[g]E_{LUMO} (vs. NHE) was calculated by $E_{HOMO} - E_{0-0}$.

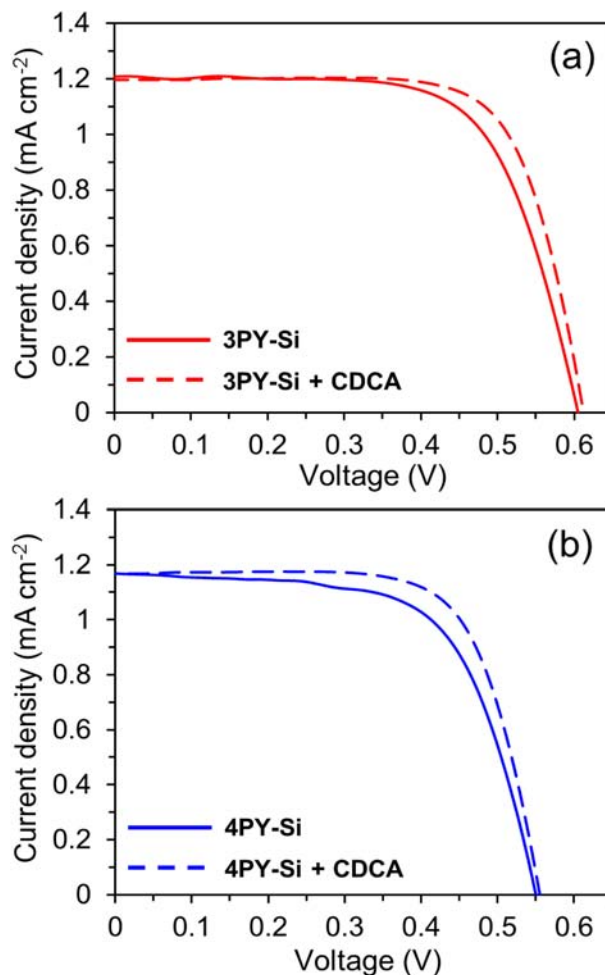**TABLE 2** Electrochemical data of **3PY-Si** and **4PY-Si**

Phthalocyanines	Redox processes	$E_{1/2}$
3PY-Si	R_1	−0.70 V
	R_2	−1.18 V
	O_1	1.23 V
4PY-Si	R_1	−0.72 V
	R_2	−1.25 V
	O_1	1.35 V

Note: All voltammetric data were given versus SCE. $E_{1/2}$ values (($E_{pa} + E_{pc}$)/2) were given versus SCE at 0.100 V s^{-1} scan rate.
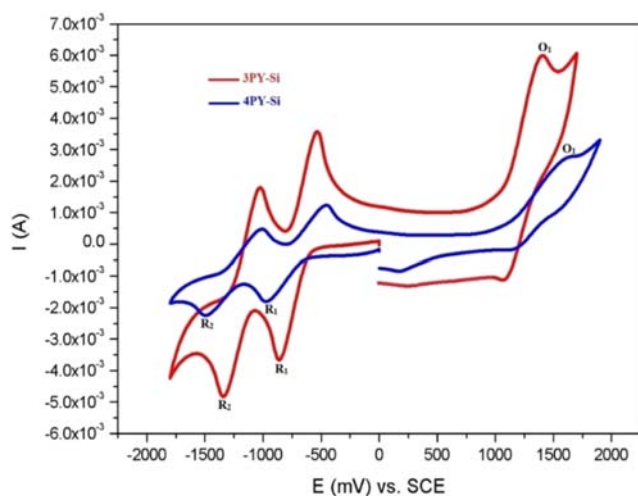
FIGURE 6 Cyclic voltamograms of **3PY-Si** and **4PY-Si** at 0.100 V s^{-1} in TBAP/DCM

FIGURE 7 *J–V* curves of the DSSCs based on (A) **3PY-Si** and (B) **4PY-Si** with or without chenodeoxycholic acid (CDCA) under AM 1.5 simulated sunlight (100 mW cm^{-2}) illumination

3.5 | Photovoltaic results

To investigate the photovoltaic properties of DSSCs based on these photosensitizers, the current density–voltage (*J–V*) curves of the DSSCs were carried out as shown in Figure 7 and the photovoltaic parameters were given in Table 3. With CDCA, the short circuit current density (J_{SC}) of 1.207 mA cm^{-2} and power conversion efficiency (PCE) of 0.48% for photosensitizer **3PY-Si**-based DSSC are slightly higher than photosensitizer **4PY-Si** (J_{SC} = 1.166 mA cm^{-2} and PCE = 0.40%). In the presence of CDCA, the dye **3PY-Si** exhibited the highest PCE of

TABLE 3 The photovoltaic results of the DSSCs with ethanol/THF (1/2) as a solvent mixture

Dye	CDCA (mM)	J_{SC}^{IPCE} (mA cm^{-2})[a]	J_{SC} (mA cm^{-2})	V_{OC} (V)	FF	PCE (%)	Dye loading amount (mol cm^{-2})
3PY-Si	0.00	1.189	1.207	0.607	0.65	0.48	2.66×10^{-8}
3PY-Si	1.00	1.202	1.208	0.611	0.72	0.53	2.49×10^{-8}
4PY-Si	0.00	1.131	1.166	0.552	0.62	0.40	2.59×10^{-8}
4PY-Si	1.00	1.139	1.168	0.556	0.67	0.44	2.38×10^{-8}

Abbreviations: CDCA, chenodeoxycholic acid; PCE, power conversion efficiency.

[a]J_{sc}^{IPCE} values were integrated from their incident photon to current conversion efficiency (IPCE) spectra.

0.53%, which is nearly 8% enhancement compared with the cell without CDCA supporting that the degree of molecular aggregations was limited.[27] It can be also seen that the J_{SC} value of **4PY-Si** is slightly lower than that of **3PY-Si**. This can explained by the LUMO level of **4PY-Si** which is slightly more negative than the CB of TiO$_2$. It is well known that the low LUMO levels led insufficient electron injections to the TiO$_2$ surface.[28]

These results exhibit that the bearing of sterically prevented substituents such as flexible and long axial pyridine groups in the photosensitizers can efficiently suppress aggregation, due to disturbance of the π–π stacking.[29] In comparison to our previous zinc phthalocyanines bearing four 3-(pyridin-3-yl)propoxy anchoring groups,[30] the lower PCEs of dyes **3PY-Si** and **4PY-Si** may be ascribed to the axial anchoring groups, which align the phthalocyanine ring planarly to the TiO$_2$ surface and reduce the amount of dye loading (Table 3). The difference in photosensitizers V_{OC} values was observed to be greater than J_{SC} values. As shown in Table 1, **3PY-Si** having the LUMO positioned 120 mV more negative to **4PY-Si** resulted in better injection thereby preventing recombination and having a higher V_{OC}.[28] Also, the J-V curves exhibit that the V_{OC} values for cells produced with CDCA are slightly amended as compared to those without co-adsorbent. The enhancement of V_{OC} can be interpreted by the co-adsorbent occupation of the bare TiO$_2$ surface in this way slightly suppress the charge recombination.[31,32]

The incident photon to current conversion efficiency (IPCE) of **3PY-Si** and **4PY-Si** devices is performed. The IPCE spectra are consistent with the absorption spectra on the semiconductor TiO$_2$ film. The devices exhibit a narrow IPCE around 675–700 nm and their IPCE peaks are limited to approximately 10%. With CDCA, the IPCE values of the DSSCs are slightly improved compared with those without CDCA which exhibits that the aggregation efficiently inhibited by the pyridine groups in the molecules (Figure 8). As expected, the values of the integrated photocurrent density (J_{sc}^{IPCE}), calculated by the integration of the IPCE spectra, are in
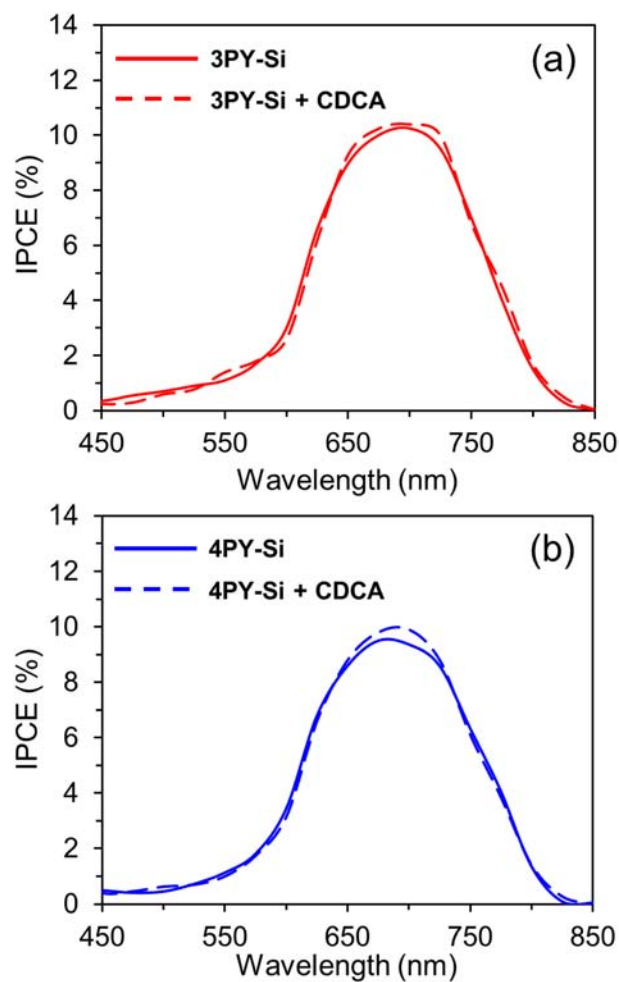

FIGURE 8 Incident photon to current conversion efficiency (IPCE) spectra of the dye-sensitized solar cells (DSSCs) based on (A) **3PY-Si** and (B) **4PY-Si** with or without chenodeoxycholic acid (CDCA) under AM 1.5 simulated sunlight (100 mW cm^{-2}) illumination

good agreement with the results of the J–V measurements (Table 3).

Electrochemical impedance spectroscopy (EIS) analysis of the DSSCs based on the dyes in the absence of CDCA were carried out in order to evaluate the interfacial charge recombination process under dark conditions.
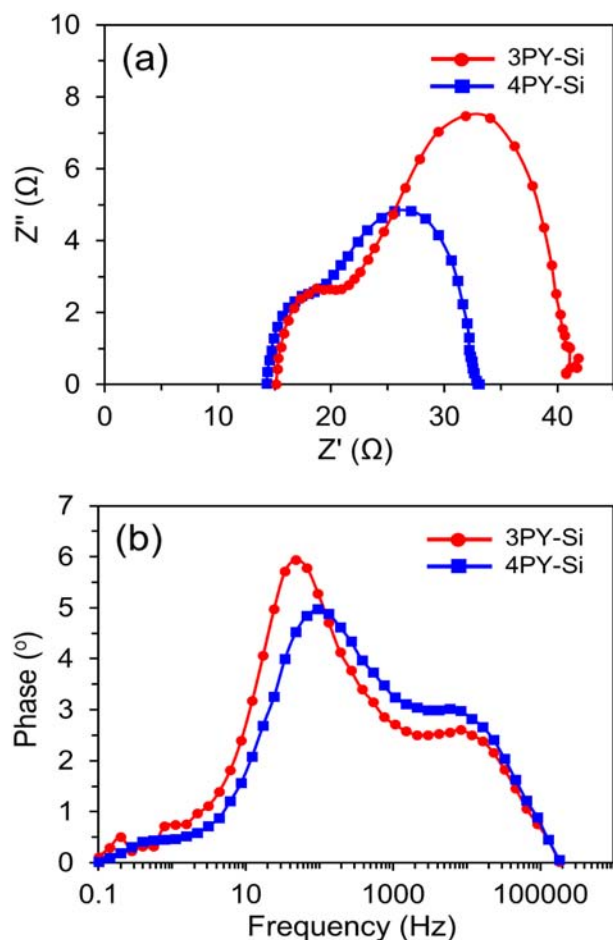
FIGURE 9 Nyquist and Bode plots of dye-sensitized solar cells (DSSCs) based on the dyes **3PY-Si** and **4PY-Si**

FIGURE 10 (A) Dark current and (B) open circuit voltage decay (OCVD) curves of the dye-sensitized solar cells (DSSCs) based on **3PY-Si** and **4PY-Si**

As shown in Figure 9A, the major semicircle in the Nyquist plots corresponds to the charge recombination resistance at the TiO_2/dye/electrolyte interface.[33,34] The radius of the major semicircle of **3PY-Si** is higher than that of **4PY-Si**, which is consistent with their V_{OC} values.[35] The electron lifetimes (τ_e), which can be calculated using the equation $\tau_e = 1/2\pi f$,[36] are 3.31 and 1.67 ms for **3PY-Si** and **4PY-Si**, which are also in agreement with V_{OC} values (Figure 9B).

The dark current reflects the reactions without illumination corresponded to the electron recombination between the electrons in the TiO_2 and the redox electrolyte. As shown in Figure 10A, the dark current for the DSSC based on **3PY-Si** smaller than that of **4PY-Si**, implying lower recombination, result in an increase of V_{OC}.[36] Figure 10B exhibits open circuit voltage decay (OCVD) curves of the cells based on the synthesized dyes. It can be seen that the decay rate of **3PY-Si** was slower than that of **4PY-Si**, which indicates that the former has a lower electron recombination rate with respect to the latter.[37]
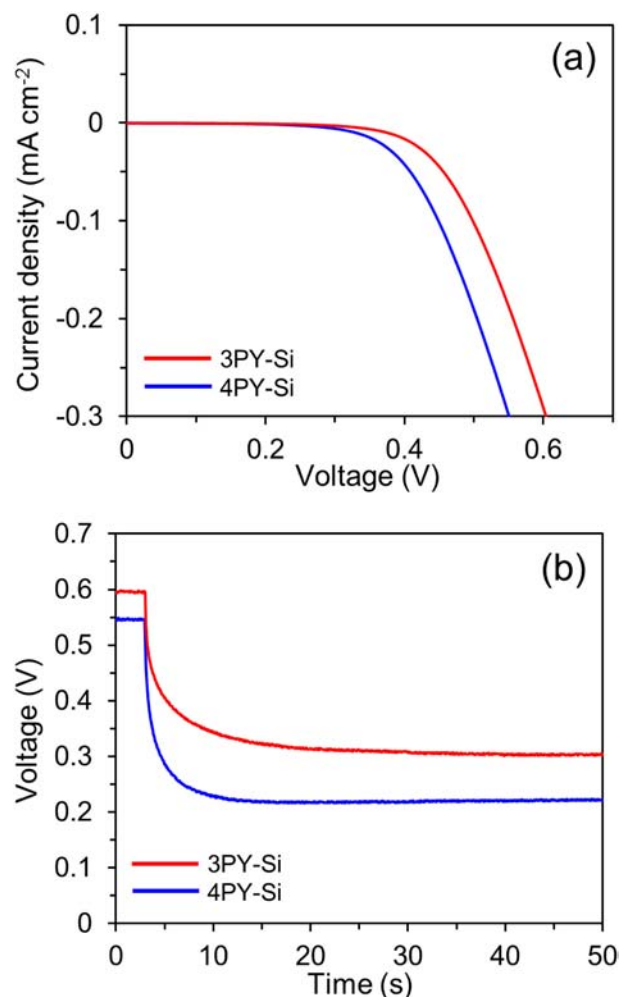
It is known that the presence of small traces of water in the redox electrolyte reduces stability of the DSSCs due to facilitating dye desorption. To evaluate this aspect, the adsorbed dyes on the TiO_2 surface were dipped in acetonitrile/water (95:5) solution and the anchoring stabilities were investigated by absorption measurements at different time intervals (Figure 11).[38] Considerably, **4PY-Si** adsorbed on TiO_2 film showed a similar drop in the absorbance with respect to that of the reference molecule **N719**. Almost identical results were also observed for **3PY-Si**. Briefly, the anchoring stability of the synthesized dyes are comparable with that of **N719**.

The long-term stabilities of the DSSCs based on **3PY-Si** and **4PY-Si** were carried out during 500 hr under simulated sunlight (Figure S6). At the end of this period, **3PY-Si** and **4PY-Si** maintained 67.9% and 65.9% of their initial PCE, respectively.
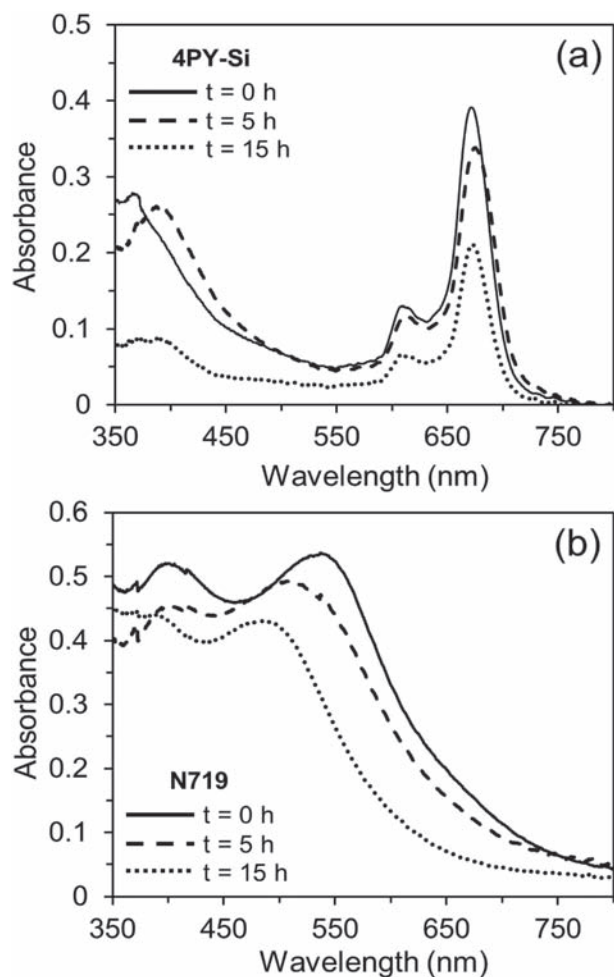
FIGURE 11 Absorption spectra of **4PY-Si** (A) and **N719** (B) sensitized nanocrystalline TiO_2 films before (t = 0 hr) and after 5 and 15 hr of desorbing treatment

4 | CONCLUSION

Herewith the new pyridine-containing substituted silicon (IV) phthalocyanine photosensitizers were prepared and evaluated as sensitizers in DSSCs. The photophysical and electrochemical studies exhibited that all the photosensitizers were suitable as anti-aggregate sensitizers for DSSCs. Fluorescence studies well performed and reasonable fluorescence quantum yield (Φ_F = 0.25) was obtained which is favorable for photophysical applications of the phthalocyanine photosensitizers. The DSSC based on complex **3PY-Si** shows the (PCE) of 0.53% with the J_{sc}, V_{oc} and FF values of 1.205 mA cm^{-2}, 0.612 V and 0.72, respectively, in the presence of the co-adsorbent. The poor performance might be resulted from the anchoring group of pyridine and non-conjugated nature of propyl moiety. The results indicate that parallel arrangement induced by the presence of anchoring groups at the axial positions of the Pc and the TiO_2 surface caused poor efficiencies, however, the central Si-

atom of the photosensitizers allows for the attachment of bulky pyridine containing groups for additional superiority such as, increasing solubility and mitigating dye aggregation which may be good photosensitizers for DSSC applications.

AUTHOR CONTRIBUTIONS
Emre Güzel: Investigation; methodology. **HÜSEYİN BAŞ:** Methodology. **Zekeriya Bıyıklıoğlu:** Investigation; methodology; supervision. **İlkay Şişman:** Methodology.

DATA AVAILABILITY STATEMENT
The data that support the findings of this study are available from the corresponding author upon reasonable request.

ORCID
Emre Güzel https://orcid.org/0000-0002-1142-3936
Hüseyin Baş https://orcid.org/0000-0002-8722-3359
Zekeriya Biyiklioglu https://orcid.org/0000-0001-5138-214X
İlkay Şişman https://orcid.org/0000-0002-0943-2817

REFERENCES
[1] M. Urbani, M. E. Ragoussi, M. K. Nazeeruddin, T. Torres, *Coord. Chem. Rev.* **2019**, *381*, 1.
[2] J. Gong, K. Sumathy, Q. Qiao, Z. Zhou, *Renew. Sustain. Energy Rev.* **2017**, *68*, 234.
[3] M. G. Chia-Yuan Chen, M. Wang, J.-Y. Li, N. Pootrakulchote, L. Alibabaei, C.-h. Ngoc-le, J.-D. Decoppet, J.-H. Tsai, C. Grätzel, C.-G. Wu, S. M. Zakeeruddin, *ACS Nano* **2009**, *3*, 3103.
[4] E. Güzel, *RSC Adv.* **2019**, *9*, 10854.
[5] J. J. Cid, M. García-Iglesias, J. H. Yum, A. Forneli, J. Albero, E. Martínez-Ferrero, P. Vázquez, M. Grätzel, M. K. Nazeeruddin, E. Palomares, T. Torres, *Chem. A Eur. J.* **2009**, *15*, 5130.
[6] B. Yıldız, E. Güzel, N. Menges, İ. Şişman, M. Kasım Şener, *Sol. Energy* **2018**, *174*, 527.
[7] I. López-Duarte, M. Wang, R. Humphry-Baker, M. Ince, M. V. Martínez-Díaz, M. K. Nazeeruddin, T. Torres, M. Grätzel, *Angew. Chemie* **2012**, *124*, 1931.
[8] H. Baş, Z. Biyiklioglu, *J. Organomet. Chem.* **2015**, *791*, 238.
[9] E. Güzel, A. Atsay, S. Nalbantoglu, N. Şaki, A. L. Dogan, A. Gül, M. B. Koçak, *Dyes Pigm.* **2013**, *97*, 238.
[10] E. Güzel, G. Yaşa Atmaca, A. Erdoğmuş, M. B. Koçak, *J. Coord. Chem.* **2017**, *70*, 2659.
[11] A. Morandeira, I. López-Duarte, B. O'Regan, M. V. Martínez-Díaz, A. Forneli, E. Palomares, T. Torres, J. R. Durrant, *J. Mater. Chem.* **2009**, *19*, 5016.
[12] M. Yanagisawa, F. Korodi, J. Bergquist, A. Holmberg, A. Hagfeldt, B. Åkermark, L. Sun, J. Porphyr, *Phthalocyanines* **2004**, *8*, 1228.
[13] Z. Biyiklioğlu, *Dyes Pigm.* **2013**, *99*, 59.

[14] Z. Biyiklioglu, D. Çakir, *Spectrochim. Acta - Part a Mol. Biomol. Spectrosc.* **2012**, *98*, 178.

[15] D. Çakir, V. Çakir, Z. Biyiklioğlu, M. Durmuş, H. Kantekin, D. Cakir, V. Cakir, Z. Biyiklioğlu, M. Durmuş, H. Kantekin, et al., *J. Organomet. Chem.* **2013**, *745–746*, 423.

[16] J. He, A. Hagfeldt, S.-E. Lindquist, H. Grennberg, F. Korodi, L. Sun, B. Åkermark, *Langmuir* **2001**, *17*, 2743.

[17] L. Zhang, J. M. Cole, *ACS Appl. Mater. Interfaces* **2015**, *7*, 3427.

[18] M. M. Mohamed, W. A. Bayoumy, M. Khairy, M. A. Mousa, *Microporous Mesoporous Mater.* **2007**, *103*, 174.

[19] Y. Ooyama, S. Inoue, T. Nagano, K. Kushimoto, J. Ohshita, I. Imae, K. Komaguchi, Y. Harima, *Angew. Chem. Int. Ed.* **2011**, *50*, 7429.

[20] M. I. Zaki, M. A. Hasan, F. A. Al-Sagheer, L. Pasupulety, *Colloids Surfaces A Physicochem. Eng. Asp.* **2001**, *190*, 261.

[21] B. Barut, Z. Biyiklioglu, C. Ö. Yalçın, M. Abudayyak, *Dyes Pigm.* **2020**, *172*, 107794.

[22] Y. Ooyama, T. Nagano, S. Inoue, I. Imae, K. Komaguchi, J. Ohshita, Y. Harima, *Chem. A Eur. J.* **2011**, *17*, 14837.

[23] E. T. Saka, M. Durmuş, H. Kantekin, *J. Organomet. Chem.* **2011**, *696*, 913.

[24] G. Y. Atmaca, C. Dizman, T. Eren, A. Erdoịmuş, *Spectrochim. Acta - Part a Mol. Biomol. Spectrosc.* **2015**, *137*, 244.

[25] T. Higashino, Y. Fujimori, K. Sugiura, Y. Tsuji, S. Ito, H. Imahori, *Angew. Chemie* **2015**, *127*, 9180.

[26] G. A. Tunç, E. Güzel, İ. Şişman, V. Ahsen, J. G. Cardenas, *New J. Chem.* **2019**, *43*, 14390.

[27] B. S. Arslan, B. Arkan, M. Gezgin, Y. Derin, D. Avcı, A. Tutar, M. Nebioğlu, İ. Şişman, *J. Photochem. Photobiol., a* **2021**, *404*, 112936.

[28] S. Soman, M. A. Rahim, S. Lingamoorthy, C. H. Suresh, S. Das, *Phys. Chem. Chem. Phys.* **2015**, *17*, 23095.

[29] Y. Ooyama, Y. Harima, *Eur. J. Org. Chem.* **2009**, *2009*, 2903.

[30] T. Keleş, Z. Biyiklioglu, E. Güzel, M. Nebioğlu, İ. Şişman, *Appl. Organomet. Chem.* **2021**, *35*, e6076.

[31] X. Kang, J. Zhang, A. J. Rojas, D. O'Neil, P. Szymanski, S. R. Marder, M. A. El-Sayed, *J. Mater. Chem. A* **2014**, *2*, 11229.

[32] B. Yıldız, E. Güzel, D. Akyüz, B. S. Arslan, A. Koca, M. K. Şener, *Sol. Energy* **2019**, *191*, 654.

[33] J. V. Vaghasiya, K. K. Sonigara, J. Prasad, M. Qureshi, S. C. Tan, S. S. Soni, *ACS Appl. Energy Mater.* **2020**, *3*(7), 7073.

[34] M. Adachi, M. Sakamoto, J. Jiu, Y. Ogata, S. Isoda, *J. Phys. Chem. B* **2006**, *110*, 13872.

[35] R. Milan, G. S. Selopal, M. Cavazzini, S. Orlandi, R. Boaretto, S. Caramori, I. Concina, G. Pozzi, *Sci. Rep.* **2017**, *7*, 1.

[36] Y. Jiao, L. Mao, S. Liu, T. Tan, D. Wang, D. Cao, B. Mi, Z. Gao, W. Huang, *Dyes Pigm.* **2018**, *158*, 165.

[37] T. B. Raju, J. V. Vaghasiya, M. A. Afroz, S. S. Soni, P. K. Iyer, *Org. Electron.* **2017**, *50*, 25.

[38] R. Grisorio, L. De Marco, G. Allegretta, R. Giannuzzi, G. P. Suranna, M. Manca, P. Mastrorilli, G. Gigli, *Dyes Pigm.* **2013**, *98*, 221.

SUPPORTING INFORMATION

Additional supporting information may be found online in the Supporting Information section at the end of this article.